

Spectra of heavy mesons in the Bethe-Salpeter approach

Christian S. Fischer^a, Stanislav Kubrak^b, and Richard Williams^c

Institut für Theoretische Physik, Justus-Liebig-Universität Giessen, 35392 Giessen, Germany

Received: 1 October 2014 / Revised: 12 December 2014

Published online: 29 January 2015 – © Società Italiana di Fisica / Springer-Verlag 2015

Communicated by R. Alkofer

Abstract. We present a calculation of the spectrum of charmonia, bottomonia and B_c -meson states with “ordinary” and exotic quantum numbers. We discuss the merits and limitations of a rainbow-ladder truncation of Dyson-Schwinger and Bethe-Salpeter equations and explore the effects of different shapes of the effective running coupling on ground and excited states in channels with quantum numbers $J \leq 3$. We furthermore discuss the status of the $X(3872)$ as a potential (excited) quark-antiquark state and give predictions for the masses of charmonia and bottomonia in the tensor channels with $J = 2, 3$.

1 Introduction

With the spectacular success of Belle, Babar, BES and the LHC experiments and their discovery of an ever-increasing and largely unexplained number of XYZ -states, hadron spectroscopy in the heavy quark region became a fascinating topic in the past years. Many of the newly discovered states are surprisingly narrow, with some of these states electrically charged and therefore not accounted for by the conventional quark model picture of quark-antiquark meson bound states. Certainly, the potential of these states to guide us in our understanding of the underlying physics of the strong interaction is enormous, as detailed, *e.g.*, in refs. [1–4] and references therein.

From a theoretical QCD perspective charmonia (and, to a perhaps lesser degree, bottomonia) are extremely interesting since they combine effects of non-perturbative QCD with perturbative concepts in the heavy quark regime. In general, the charm quark is not heavy enough to be considered as non-relativistic. Thus especially excited states in the charmonium spectrum have to be considered in a framework that is genuinely relativistic or, at least, incorporates relativistic corrections. Model calculations in terms of relativistic quasipotentials reproduce many features of the spectrum [5–8] and provide important guidance on the structure of the spectrum. However, in order to gain a more systematic understanding of the underlying physics of the strong interaction it is mandatory to employ approaches that are directly rooted within QCD. At least two different strategies have been employed in this

direction. On the one hand, lattice gauge theory as well as non-relativistic QCD (NRQCD) and potential NRQCD have made substantial progress in determining the details of the heavy quark potential from QCD [9–11].

On the other hand, the heavy quarkonia states can be directly calculated from the underlying QCD Lagrangian without the need to resort to expansions in terms of quark velocities or heavy quark masses. Such approaches have the obvious advantage that the heavy and the light quark sectors can be treated in the same framework. In the charmonium sector, lattice gauge theory has made an ever increasing effort to determine the spectrum of ground and excited states as well as exotics in dynamical calculations, see, *e.g.*, [12–16] and references therein as well as [19, 20] for short reviews.

An alternative approach based on QCD is the relativistic functional framework employing the Dyson-Schwinger and Bethe-Salpeter equations. Within the rainbow-ladder approximation first studies of the quarkonium spectrum [21–24] as well as exotic states like tetraquarks [25] in the heavy quark region have been performed, accompanied by systematic studies in the limit of static quarks [26–28].

In this work we refine and extend these calculations in two directions. On the one hand we include states with higher angular momentum up to $J = 3$. On the other hand we perform a systematic study of the influence of details in the momentum dependence of the underlying effective running coupling on the spectrum of ground and excited states in these channels. We extend our analysis of [29] to the heavy $\bar{c}c$, $\bar{b}b$ and $\bar{b}c$ mesons. In the process, we generalize the frequently used the Maris-Tandy interaction in order to explore the impact of the shape of the interaction, with an emphasis on the resultant splitting between different meson channels and their excited states.

^a e-mail: christian.fischer@physik.uni-giessen.de

^b e-mail: stanislav.kubrak@theo.physik.uni-giessen.de

^c e-mail: richard.williams@theo.physik.uni-giessen.de

The paper is organized as follows. In sect. 2 we summarize the framework of the DSE and BSEs, together with a discussion of the rainbow-ladder interaction employed. Our results are presented and discussed in sect. 3. We conclude in sect. 4.

2 Framework

We work with the one-particle irreducible Green's functions of QCD in Euclidean space, obtained through solutions of their corresponding Dyson-Schwinger equations (DSEs).

With the quark propagator decomposed as

$$S^{-1}(p) = Z_f^{-1}(p^2) (i\not{p} + M(p^2)) , \quad (1)$$

where $Z_f(p^2)$ is the quark wave function and $M(p^2)$ its mass function, we solve its DSE

$$S^{-1}(p) = Z_2 S_0^{-1}(p) + g^2 Z_{1f} C_F \int_k \gamma^\mu S(k+p) \Gamma^\nu(k+p, p) D_{\mu\nu}(k). \quad (2)$$

For brevity, we write $\int_k = \int d^4k/(2\pi)^4$. The bare propagator, $S_0^{-1}(p)$ is obtained from eq. (1) by setting $Z_f(p^2) = 1$ and $M(p^2) = m_0$, with m_0 related to the renormalized quark mass m_q by $m_0 = Z_m m_q$. The renormalized coupling of QCD is denoted by $\alpha = g^2/(4\pi)$ and Z_2 , Z_m and Z_{1f} are the renormalisation factors of the quark wave function the quark mass and the quark-gluon vertex. Colour traces yield the Casimir factor $C_F = 4/3$.

The non-trivial inputs into the quark DSE are the gluon propagator $D_{\mu\nu}(k)$, and the dressed quark-gluon vertex $\Gamma^\nu(k, p)$. Since we work in Landau gauge the gluon propagator is transverse and given by

$$D_{\mu\nu}(k) = T_{\mu\nu}(k) \frac{Z(k^2)}{k^2}, \quad (3)$$

where $T_{\mu\nu}(k) = \delta_{\mu\nu} - k_\mu k_\nu / k^2$ is the transverse projector. We will discuss the quark-gluon vertex and the details of our truncation below.

Bound states of a quark and an antiquark are described by the (homogeneous) Bethe-Salpeter equation for the corresponding Bethe-Salpeter amplitude $\Gamma(p; P)$

$$[\Gamma(p; P)]_{tu} = \lambda(P_i^2) \int_k K_{tr;su}^{(2)}(p, k; P) [S_+ \Gamma(k; P) S_-]_{rs}, \quad (4)$$

with a discrete spectrum of solutions found at $P^2 = -M_i^2$ for eigenvalues $\lambda(P_i^2) = 1$. The quarks $S_\pm = S(k_\pm)$ carry momentum $k_\pm = k + (\xi - 1/2 \pm 1/2)P$ with momentum partitioning ξ . Since the equation is manifestly covariant, all solutions are independent of ξ . The quantum numbers of the bound state under consideration follow from the tensor structure of $\Gamma(p; P)$. The two-particle irreducible quark anti-quark interaction kernel $K_{tr;su}^{(2)}(p, k; P)$ is chosen to be consistent with eq. (2) and the axial-vector

Ward-Takahashi identity such that the chiral properties of the pion are preserved: the pion is both a bound state of a quark and an antiquark and a massless Goldstone boson in the chiral limit.

2.1 The rainbow-ladder approximation

In the rainbow-ladder truncation scheme one replaces the combined effects of the dressed gluon propagator and dressed quark-gluon vertex by a one-gluon-exchange model with effective coupling and bare vertex. In the light quark sector the most important merit of the rainbow-ladder scheme is its compliance with chiral symmetry such that the (pseudo-)Goldstone boson nature of the pseudoscalar mesons and the associated Gell-Mann–Oakes–Renner relation are satisfied. In the opposite limit of very heavy quarks it has the (perhaps surprising) tendency to become exact [26–28]. For realistic masses of the charm and bottom quarks the static limit is relevant in the sense that potentials using the vector structure of one-gluon exchange only are able to reproduce global features. Nevertheless, when it comes to the quantitative details such as the spin-orbit splitting, sizeable corrections occur. On the other hand, it has been argued in [30] that the constraints of chiral symmetry still play an important role in the heavy quark region. We conclude from this that systematic studies of the feasibility of the rainbow-ladder scheme in the heavy quark region provide an important systematic link between the chiral and the static limit of QCD. We will see that our study nicely complements our ref. [29] where we have elucidated the assets and shortcomings of the rainbow-ladder scheme for the spectrum of light quarks. Here we provide a similar analysis for heavy quarks.

In the rainbow-ladder scheme the quark-gluon interaction appearing in the quark DSE is combined into an effective interaction $\alpha_{\text{eff}}(q^2)$

$$Z_{1f} g^2 D_{\mu\nu}(k) \Gamma_\nu(k+p, p) \rightarrow 4\pi Z_2^2 T_{\mu\nu}(k) \frac{\alpha_{\text{eff}}(k^2)}{k^2} \gamma_\nu, \quad (5)$$

with the appearance of Z_2^2 following from the Slavnov-Taylor identities to maintain multiplicative renormalizability.

The corresponding symmetry-preserving two-body kernel is given by

$$K_{tr;su}^{(2)} = 4\pi Z_2^2 \frac{\alpha_{\text{eff}}(k^2)}{k^2} T_{\mu\nu}(k) [\gamma^\mu]_{tr} [\gamma^\nu]_{su}. \quad (6)$$

One of the most frequently used examples of an effective quark-gluon interaction is that of Maris and Tandy [31]. It consists of a term which guarantees the correct ultraviolet behaviour of the quark-DSE according to one-loop resummed perturbation theory and a term which is only active in the infrared and supplies enough interaction strength to trigger chiral symmetry breaking. The interaction can be represented by

$$\alpha_{\text{eff}}(q^2) = \alpha_{\text{IR}}(q^2) + \alpha_{\text{UV}}(q^2), \quad (7)$$

where

$$\alpha_{\text{IR}}(q^2) = \pi\eta^7 \mathcal{P}(x) e^{-\eta^2 x}, \quad (8)$$

$$\alpha_{\text{UV}}(q^2) = \frac{2\pi\gamma_m (1 - e^{-y})}{\ln[e^2 - 1 + (1 + z)^2]}, \quad (9)$$

with momenta $x = q^2/\Lambda^2$, $y = q^2/\Lambda_t^2$, $z = q^2/\Lambda_{\text{QCD}}^2$. Here $\mathcal{P}(x)$ is a general polynomial that is equal to x^2 in the original Maris-Tandy model. Below we will also discuss modifications of $\mathcal{P}(x)$. Typically Λ is constrained in the light quark sector to be equal to 0.72 GeV by matching this scale to the known value of the pion leptonic decay constant. Some results for ground states are then found to be insensitive to the dimensionless parameter η , whereas the masses of the excited states in general depend much more strongly on this parameter.

In addition, this setup ignores the flavour dependence of the quark-gluon interaction. For heavy quarks, recent results on the quark-gluon vertex suggest a considerable decrease in the dressing effects when the quark mass becomes heavy [32], a result in accordance with the general considerations from the beginning of this subsection. As a consequence, one would expect Λ and η to differ in the effective interaction for light and heavy hadron states. More generally one could expect the shape of the interaction to change, hence the generalization in eq. (8) to feature $\mathcal{P}(x)$. Below we therefore employ the polynomial form,

$$\mathcal{P}(x) = \sum_{i=1}^n a_i x^i, \quad (10)$$

and investigate its impact on the heavy meson spectrum restricting ourselves to terms with $n \leq 4$.

2.2 Numerical methods

Our numerical methods have been explained in ref. [29] and we refer the reader to this work for details. For the quark-DSE we use a version where the complex momentum is flowing through the internal quark propagator, leaving the momentum in the Maris-Tandy interaction real. This way we avoid the sizable numerical errors that may occur when evaluating the effective interaction in the complex plane. Furthermore we use a Pauli-Villars-type regulator to avoid cut-off effects in the quark-DSE.

In general, when evaluating bound state in channels with large angular momentum J or radially excited states the problem arises that the Bethe-Salpeter equation evaluates the internal quark propagators at large time-like momenta. With increasing mass of the state in question at some point one probes the analytic structure of the quark propagators, which in rainbow-ladder approximation is given by pairs of complex conjugate poles [33–35]. Since the numerical treatment of the quark-DSE at and beyond these poles is extremely hard we refrain from a brute force treatment of the problem and resort to the extrapolation techniques for the eigenvalue of the BSE described in ref. [29]. There we compared two different

extrapolation techniques and estimated thereby the associated error. For ground states with masses not too far beyond the calculable domain, these errors are generically on the level of 1%. For excited states and states with larger masses the accumulated error of extrapolation is larger. We accepted extrapolations up to errors on the 5% level for the exploratory study presented here.

3 Results

3.1 Charmonia

3.1.1 Vanilla Maris-Tandy

We start our study with what we term the vanilla Maris-Tandy interaction, *i.e.* we keep the scale $\Lambda = 0.72$ GeV from the light meson sector and explore the dependence of the spectrum on η . Furthermore, for the polynomial $\mathcal{P}(x)$ in eq. (8) we use the Maris-Tandy form ($a_2 = 1$, remaining $a_i = 0$). This original form of the Maris-Tandy (MT) interaction has been employed in the heavy meson sector already in ref. [22]. It therefore provides a convenient starting point. In the subsections 3.1.2, 3.1.3 and 3.1.4 below, we will also discuss deviations from this form in a_1 , a_4 or the scale Λ .

In ref. [22] a general fit has been performed of ground state masses in the vanilla MT model to experimental values. Here we employ a different strategy. We utilise an observation made in [29], namely that the channels 1^{--} , 2^{++} , 3^{--} , etc., are particularly well represented in the rainbow-ladder framework. Within the realms of potential quark models these states share the property that the spin-spin tensor forces do not play an important role. Since these states are well represented in the vanilla MT interaction in the light meson sector, we first concentrate on the ground and first excited state in the 1^{--} -channel (J/Ψ , $\Psi(2s)$) and the ground state in the 2^{++} -channel (χ_{c2}). We minimize the deviations of our calculated masses with the experimental values under variation of the charm quark mass and the η -parameter in the MT interaction. We obtained good agreement with experiment using a charm quark mass of $m(19 \text{ GeV}) = 0.870$ GeV and a value $\eta = 1.157$.

Our results for all presently available channels are shown in fig. 1, the explicit values are all collected in table 1 at the end of the results section. Since we have fixed the two input parameters from J/Ψ , $\Psi(2s)$ and χ_{c2} , all other states can be viewed as model predictions. In the pseudoscalar channel we find a mass of the η_c which is slightly too low, but still within 3% of the experimental value. In the language of potential models, this may indicate an overestimation of the spin-spin contact term in the effective interaction. Very good agreement with experiment is obtained for the ground state in the 1^{++} -channel, whereas the masses of the scalar 0^{++} and the axialvector 1^{+-} ground states are further off but still within five percent of the experimental value. Similar results have been obtained already in refs. [22, 23]. The new element here is the calculation of states with $J = 3$ and the excited

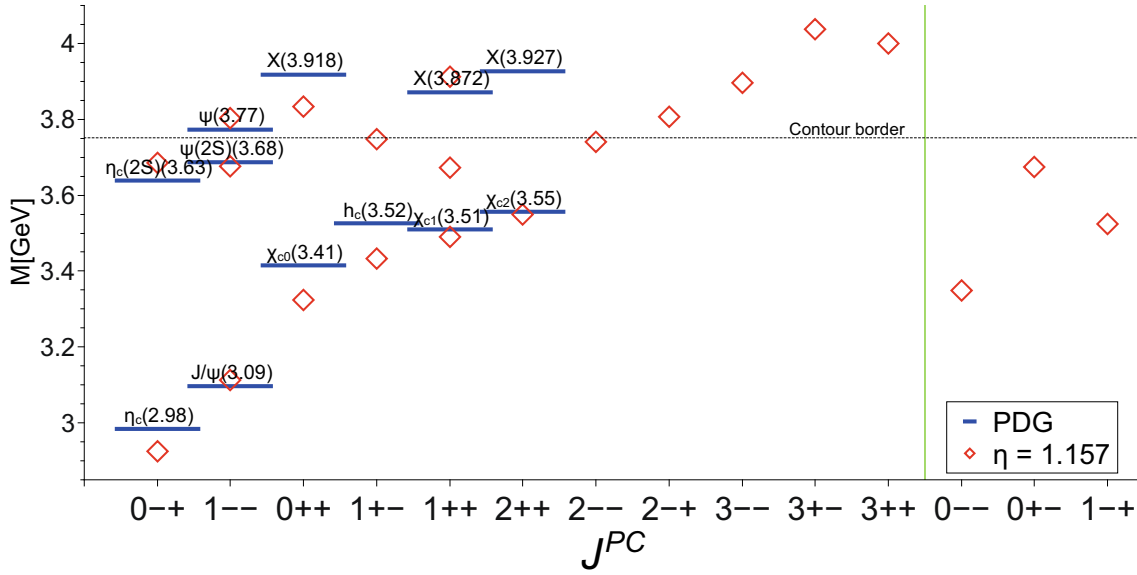


Fig. 1. Spectrum of ground and excited charmonium states for vanilla MT-rainbow-ladder interaction. The three rightmost states are exotic in the quark-model.

Table 1. Calculated masses for ground and excited charmonium, bottomonium and charm-bottom states.

J^{PC}	$c\bar{c}$			$b\bar{b}$			$b\bar{c}$	
	$n = 0$	$n = 1$	$n = 2$	$n = 0$	$n = 1$	$n = 2$	J^P	$n = 0$
0^{-+}	2925	3684		9414	9987		0^+	$6714^{+67.1}_{-67.1}$
0^{--}	3348			9642			0^-	$6354^{+23.5}_{-23.5}$
0^{++}	3323	3833		9815	10254		1^+	
0^{+-}	3674			10014			1^-	$6498^{+64.9}_{-64.9}$
1^{-+}	3524			9788				
1^{--}	3113	3676	3803	9490	10089	10327		
1^{++}	3489	3672	3912	9842	10120	10303		
1^{+-}	3433	3747		9806	10154			
2^{-+}	3806			10194				
2^{--}	3739			10145				
2^{++}	3550			9906				
3^{--}	3896			10232				
3^{++}	3999			10302				
3^{+-}	4037			10319				

states. In ref. [29] we already observed in the light quark sector, that the rainbow-ladder interaction is well suited to reproduce states in the sequence 1^{--} , 2^{++} , 3^{--} , \dots , which are located on the same Regge-trajectory. Since we reproduce the experimental results for the J/ψ and the χ_{c2} with an error below 1%, we therefore expect our result for the mass of the 3^{--} -state of

$$m_{3^{--}} = 3896 \text{ GeV} \quad (11)$$

to be also accurate on this level due to uncertainties in the interaction alone. Since this state is a ground

state beyond but still close to the boundary of calculable states (the dashed line in the plot) it is not subject to a large extrapolation error (see [29] for a discussion of the extrapolation procedure). We therefore expect our prediction for the mass of this state to be quite robust, with a guesstimate of the overall error on the 3% level. Within these errors, we agree with the quark model prediction [7] and the lattice QCD results [13, 14]. For the other tensor ground states with $J = 2$ and $J = 3$ we expect our results to be much less accurate, with a guesstimate of total systematic errors on the 5–10% level.

Similar to the light quark sector [29] we also find, that the sequence 1^{--} , 2^{++} , 3^{--} lies on a Regge trajectory with an accuracy that is even better than in the potential model of ref. [7]. For $J = \alpha M^2 + \alpha_0$ we find $\alpha = 0.36$ and $\alpha_0 = -2.55$, which is also somewhat steeper than the result of [7]. For the heavy quark sector this confirms a result found in ref. [29] for light quarks, that Regge-type behaviour in the spectrum may be found without any direct connection to an underlying string picture.

We also calculated the masses of ground states with exotic quantum numbers that cannot be accounted for as $q\bar{q}$ -states in quark models. Our results are displayed in fig. 1. Note that within a genuinely relativistic framework such as lattice QCD or the functional approach used here, there is no problem representing these states with bilinear operators. Therefore they naturally appear also in the $q\bar{q}$ spectrum. Of course, it is then an open question, whether sizeable admixtures from states with a different quark content than $q\bar{q}$ (captured only in appropriate extensions of the quark-gluon interaction beyond rainbow ladder) do exist. Furthermore, even within the $q\bar{q}$ picture large corrections beyond rainbow ladder may occur. Because of these possibilities our calculated masses should be regarded with a lot of caution.

For the excited states we observe very good agreement in the vector channel: our value for the mass of the $\Psi(2S)$ is very close to the experimental one, and even the next radial excitation is nicely represented. In the pseudoscalar channel the splitting between the ground and the excited state is slightly too large, making the agreement of the $(2S)$ -state with experiment even better than for the ground-state η_c . It is interesting to observe that the resulting fine structure splitting of the ground and excited states show a qualitatively difference when compared with experiment: whereas the ground-state splitting is too large the splitting in the excited state is too low. Such an uncorrelated behaviour of the two splittings has also been observed in lattice QCD [13].

In the “good” tensor channel 2^{++} potential radially excited states like the $X(3927)$ are not reproduced in our framework. There is a considerable uncertainty due to the extrapolation procedure needed in this mass region (see the discussion in sect. 2.2), which is enhanced for excited states. Taking our result at face value, however, the current model would disregard the notion of the $X(3927)$ to be an ordinary meson state.

From an experimental point of view, the 1^{++} -channel is perhaps the most interesting one. There the famous $X(3872)$ -state awaits its identification as a meson-molecule, a tetraquark, or an ordinary quark-antiquark bound state. The literature on this subject is enormous, therefore we point the reader only to ref. [4] for a first overview. The interesting question in this context is whether a description on a quark-antiquark basis is possible at all for the $X(3872)$. In the present rainbow-ladder model we find a ground state in this channel that is only slightly below the experimental state χ_{c1} . In addition, we find an excited state at $m = 3672$ MeV that cannot be accounted for by experiment. A second excitation is found at $m = 3912$ MeV, close to the quark model pre-

diction for the first radial excitation. Indeed, we verified by inspection that the Bethe-Salpeter wave function of our second excitation corresponds to the first radial excitation, have one zero crossing at finite relative momentum between the quark-antiquark constituents. Thus we agree with the quark-model result, that the splitting between ground state and first radial excitation in the 1^{++} -channel is too large to account for the $X(3872)$ to be a pure radially excited quark-antiquark state. This is true for the vanilla MT interaction, but we will argue below that modifications of the interaction within the rainbow-ladder framework do not change this situation. What remains to be clarified is the nature of the extra state that we see at $m = 3672$ MeV. We verified that the leading part of its wave function has no zero crossing, thus ruling out its interpretation as a radial excitation. It has well-defined charge conjugation and parity properties, but it cannot be accounted for by the naive quark model picture.

Currently, we do not have a good explanation for the appearance of this state. In principle, it may or may not be that this state is spurious in the sense that it only appears in the rainbow-ladder framework and disappears when corrections beyond rainbow ladder are taken into account. Clearly, the present form of the rainbow-ladder interaction is not sufficient to describe all structures of the experimental spectrum. This is especially apparent in the 0^{+-} - and 1^{+-} -channels. We therefore expect sizeable corrections when interactions beyond the rainbow-ladder approximation are taken into account¹. This is the subject of future work. Here, as a first step in this direction, we would like to explore the extent to which the rainbow-ladder interaction can be modified to improve the agreement with experiment. To this end we systematically explore the variations of the spectrum once we go away from the simple shape of the effective coupling eq. (7) with polynomial $\mathcal{P}(x) = x^2$, *i.e.* $a_2 = 1$ and all other $a_i = 0$ in eq. (10). This is the subject of the next two subsections.

3.1.2 Effective interaction including a_1

In order to study the variations of the charmonium spectrum with respect to changes in the general momentum behaviour of the effective coupling we now introduce additional structure in the polynomial $\mathcal{P}(x)$ in eq. (8). First we vary a_1 in the interval $-0.5 \leq a_1 \leq 0.5$. For the effective running coupling the resulting variation is shown in fig. 2. Clearly, the integrated strength, but also the fine details of the coupling change: For negative a_1 we even obtain a zero crossing with the corresponding scale associated with the relative strength between the a_1 - and a_2 -terms (here we keep $a_2 = 1$). Such an effective coupling is unusual, but not unreasonable. Recent calculations of the three-gluon vertex [36–38] suggest that the interplay between ghost and gluon degrees of freedom in the corresponding Dyson-Schwinger equation for the vertex may very well introduce such a zero crossing. This possibility is also seen in corresponding lattice calculations [39].

¹ In addition, for states above the $D\bar{D}$ -threshold coupled-channel effects may play an important role.

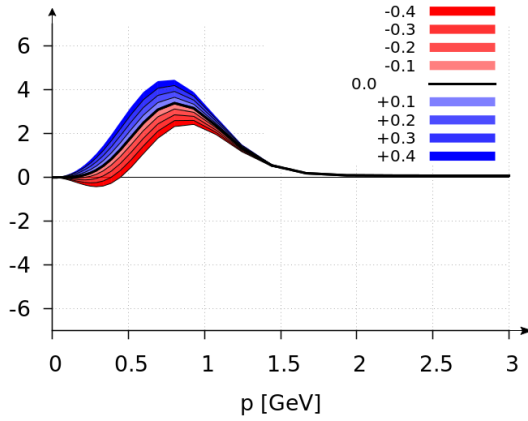


Fig. 2. The shape of the effective coupling for the generalized Maris-Tandy interaction with varying a_1 and $a_2 = 1$ held constant (see text for further explanations).

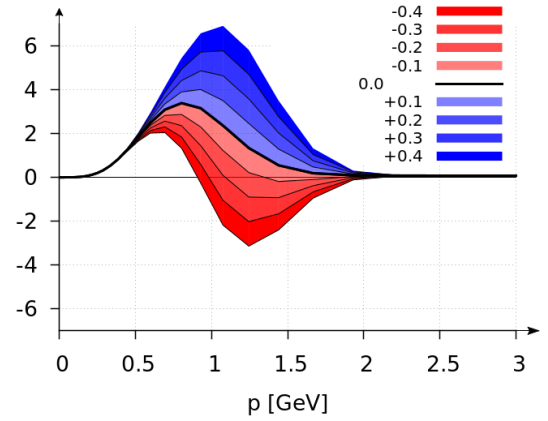


Fig. 4. The shape of the running coupling for the generalized Maris-Tandy interaction with $a_2 = 1$, $a_1 = a_3 = 0$ and varying a_4 .

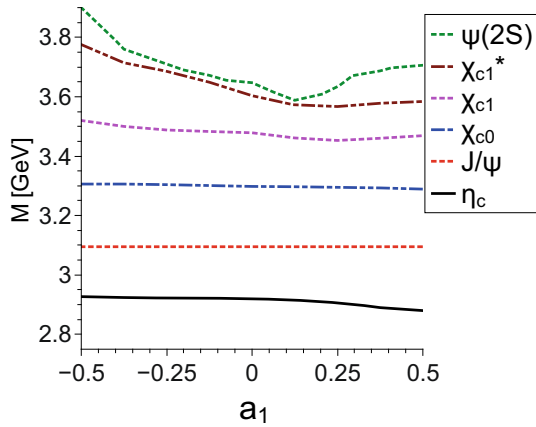


Fig. 3. The response of masses of bound and excited states on the variation of the shape of the effective interaction with a_1 .

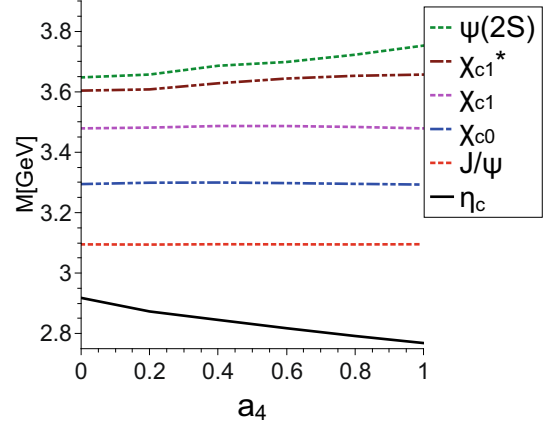


Fig. 5. The response of masses of bound and excited states on the variation of the shape of the effective interaction with a_4 .

Since the three-gluon vertex is an integral part of the non-Abelian diagrams in the DSE for the quark-gluon vertex, this behaviour may translate into a corresponding zero crossing of the quark-gluon vertex [32] and subsequently into the effective coupling.

The resulting changes in the meson spectrum are displayed in fig. 3. Adjusting the bare charm quark mass via $m_{J/\Psi}$ to accommodate for the changes in the integrated interaction strength we observe only very small changes in the resulting masses for the ground-state mesons. However, the excited states turn out to be sensitive to the details of the interaction. This is particularly true for the $\Psi(2S)$ and the first excitation in the 1^{++} -channel, which we denoted by χ_{c1}^* in order to distinguish it from the second excited state in this channel which we identified with the first radial excitation χ'_{c1} as discussed above. In particular for negative values of a_1 , corresponding to the zero crossing of the interaction discussed above, we find much increased values for the mass of the χ_{c1}^* , which eventually may even hit the experimentally observed mass of the $X(3872)$. However, this comes at a price: the mass of the $\Psi(2S)$ reacts in a similar way and substantially moves away from the experimental value, almost reproduced for $a_1 = 0$. In general we find that variations of the infrared

behaviour of our interaction via changes in a_1 do not improve the agreement of the calculated spectrum with the experimental one.

3.1.3 Effective interaction including a_4

Next we consider the generalized Maris-Tandy interaction, eq. (8), given by $a_1 = 0$, $a_2 = 1$ but non-trivial components a_3 or a_4 . Both of these modify the interaction in the intermediate momentum region, while keeping the infrared and ultraviolet behaviour untouched as can be seen from fig. 4 for the example of variations in a_4 . Since variations of a_3 act similarly on the effective coupling we keep $a_3 = 0$ fixed and restrict ourselves to variations of a_4 . Furthermore, we keep $a_4 \geq 0$, since there are no indications that the dressing of the quark-gluon vertex can induce a negative effective interaction in the mid-momentum region (in contrast to the infrared momentum region discussed in sect. 3.1.2 above).

Again, we study the variation of the charmonium spectrum while still readjusting the charm quark mass to reproduce the vector ground-state J/Ψ . Our results are given in fig. 5. Here we find a substantial increase in the mass splitting between the pseudoscalar and the vector

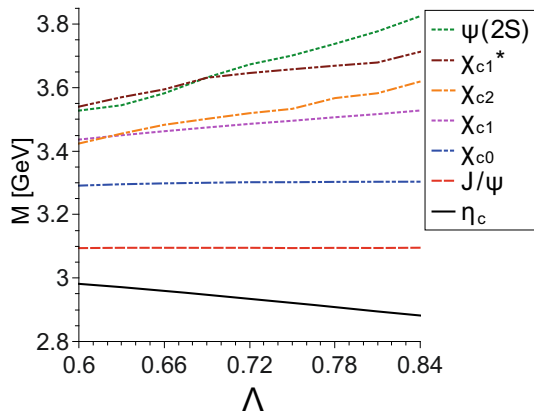


Fig. 6. The response of masses of bound and excited states on the variation of the scale parameter Λ in the interaction.

channel due to the additional interaction strength in the mid-momentum region. At the same time, the masses of the excited states $\Psi(2S)$ and χ_{c1}^* increase slightly. This moderate increase is, however, nowhere large enough to bring the χ_{c1}^* close to the observed $X(3872)$ -state. In general we find that variations of the mid-momentum behaviour of our interaction via changes in a_4 do not improve the agreement of the calculated spectrum with the experimental one.

3.1.4 Vanilla Maris-Tandy with variation of Λ

Finally we studied the variation of the masses of the ground and excited states with a change of the scale Λ in the interaction. We varied the scale between $0.6 \text{ GeV} \leq \Lambda \leq 0.84 \text{ GeV}$, keeping $\eta = 1.157$ fixed but readjusting the charm quark mass such that the ground state in the vector channel does not change. Our results are shown in fig. 6. We find a substantial variation in particular of the mass of the first excited state in the vector channel with change of Λ . This variation is so steep, that the agreement with the measured mass is only good in the vicinity of the scale $\Lambda = 0.72 \text{ GeV}$ inherited from the light meson sector in the first place. This justifies our original choice in sect. 3.1.1.

3.2 Bottomonia

Our results for the spectrum of bottomonia are shown in fig. 7. Compared to the charmonium spectrum in fig. 1 we had to change the shape of the interaction by adjusting the η -parameter from $\eta = 1.157$ for the charm case to $\eta = 1.357$ for the bottom quarks. This reflects part of the underlying flavour dependence of the quark-gluon interaction as noted in ref. [32]. Our corresponding mass of the bottom quark is $m(19 \text{ GeV}) = 3.790 \text{ GeV}$. The resulting spectrum of ground and excited states, however, has similar features when compared with experimental values as the charmonium one. Once again, the 0^{-+} , 1^{-} and 2^{++}

ground states are well represented. The necessary extrapolation needed for the 2^{++} is still under control, since the state is not too far above the limit where everything can be calculated (the dashed line in the plot). Surprisingly good is also the negative parity tensor state, although the extrapolation procedure in this mass region must be considered with a little more caution. The ground states in the scalar and axial vector channels are further off their experimental counterparts, although still within the 1% deviation margin. Thus overall, the ground-state spectrum of bottomonia is well represented in the rainbow-ladder approximation of the BSEs. Provided the good agreement in the 2^{--} -channel can be seen as an indication that extrapolation even in this mass region works well, we can regard the masses of the further tensor states with $J = 2$ and $J = 3$ as more or less solid predictions on the level of one percent. Compared to the quark-model predictions of [7] we find only slight deviations of the order of 30–70 MeV for the 2^{-+} and the states with $J = 3$.

In contrast to the charm case, the lowest-lying excited states in the bottomonium spectrum are already in a mass region where we need to extrapolate the eigenvalue of the BSE, as discussed above. Nevertheless, the extrapolation procedure seems to work and the results are surprisingly good and comparable with the corresponding ones in the charmonium spectrum, where much less extrapolation was needed. The first excited states in the pseudoscalar, vector and even the scalar channel are quite accurate and even the $\Psi(3S)$ works reasonably well. In the 1^{++} -channel we make the same observation as in the charmonium spectrum: there is a first excited state which is not a radial excitation, whereas the second excited state can be identified with the first radial excitation in the channel, *i.e.* the χ'_{b1} . Again, it will be interesting to study corrections beyond the rainbow-ladder framework.

Our results for exotic states are also given in the plot, although, as already mentioned for the charmonia spectrum, they should be regarded with some caution due to potential mixing effects with non- $q\bar{q}$ -states in these channels.

3.3 Charm-bottom bound states

Finally, we present our results for selected channels of B_c -mesons. Heavy-light systems in the Bethe-Salpeter approach are notoriously difficult to treat, since the problem of probing the analytical structure of the internal quark propagators already appears for ground states, see, *e.g.*, refs. [40, 41] for recent studies of the problem. Our results for these states, shown in fig. 8 are therefore all extrapolated and have a systematic error of about 5–10%. In the plot we show values obtained using a variation of the η -parameter in the interaction ranging approximately between the ones used for the charmonia and bottomonia. In this way we heuristically take into account the varying strength of the interaction for the two different quark flavours involved. The central value, given by the red line, corresponds to $\eta = 1.257$. Given the inherent uncertainties in the calculation, our value for the B_c in

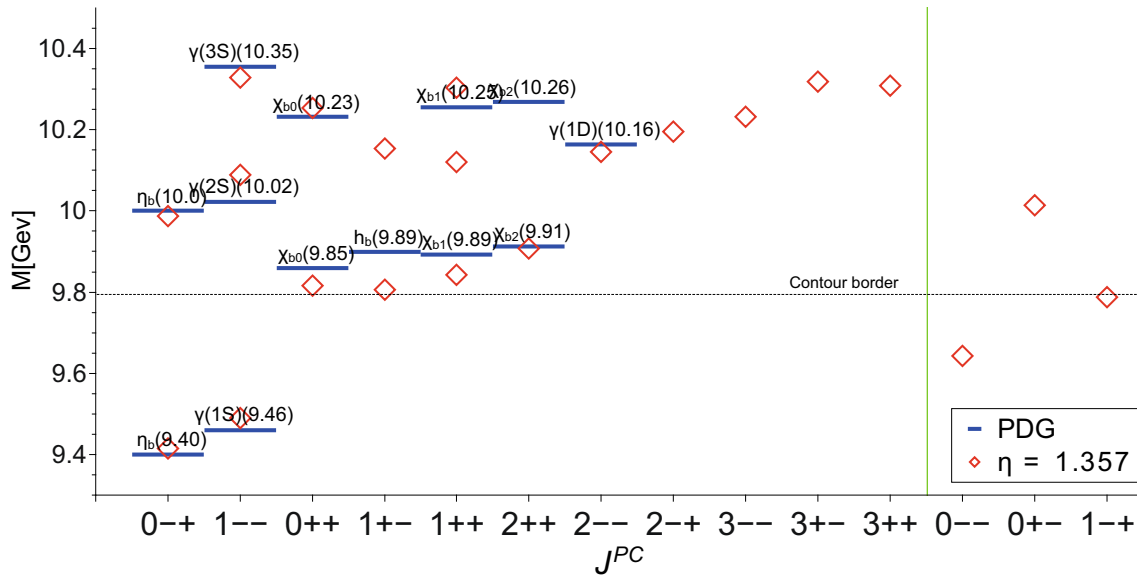


Fig. 7. Spectrum of ground and excited bottomonium states for the vanilla MT-rainbow-ladder interaction. The three rightmost states are exotic in the quark-model.

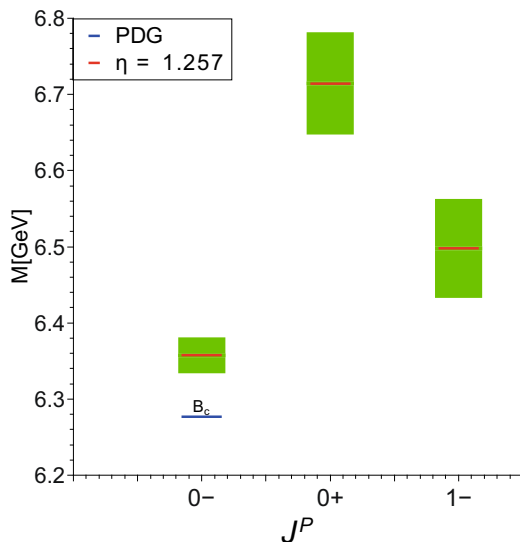


Fig. 8. The calculated $b\bar{c}$ spectrum compared to experiment. The green bands correspond to the variation $\eta = 1.257 \pm 0.1$.

the pseudoscalar channel is surprisingly close to the experimental one. Since this is the state with the lowest mass, the extrapolation error is also smallest. Since the rainbow-ladder approach works well in the vector channel we consider the existence and to some extent also the mass of the vector state as a prediction of the approach, whereas the scalar channel has to be considered with much more reservation. Despite these sources for errors it is interesting to note that our results for all three states agree qualitatively with the ones in the relativistic quark model of ref. [7] with quantitative deviations of at most 3%.

4 Summary and conclusions

In this work we presented a first calculation of ground and excited states with angular momentum $J \leq 3$ in the heavy quark sector using the framework of Dyson-Schwinger and Bethe-Salpeter equations. We have used a simple interaction model, the rainbow-ladder approximation, which is known to represent only part of the complicated interaction pattern of quarks and gluons even for heavy quarks. Nevertheless, we obtained surprisingly good results, at least for selected quantum numbers. In general, the systematics in the spectrum for charmonia and bottomonia is very similar, although the underlying interaction is not the same. Compared to the light quark sector, where the rainbow-ladder approximation has clear deficiencies [29], the agreement with the experimental states is much improved. This is particularly true for the ground and excited charmonia and bottomonia states in the vector channel, where even the second radial excitation is well represented. For pseudoscalar states and tensor states with quantum number 2^{++} we obtain reasonable results, whereas for scalars and axialvectors some deviations occur. We also gave predictions for the other tensor states, in particular for the 3^{--} , which should be a channel where the rainbow-ladder approximation does particularly well. For the bottomonia, our values for the tensor states may be considered as solid predictions for experiment with a systematic error due to extrapolations on the 1% level. We also gave results for B_c states and quarkonia with exotic quantum numbers, although the accumulated errors in these channels due to deficiencies in the rainbow-ladder interaction may be sizeable.

Furthermore, we studied variations of the shape of the rainbow-ladder effective coupling with the aim to explore whether the first or second excitation in the 1^{++} -channel can be linked to the $X(3872)$ without destroying other

parts of the spectrum. It turned out, that this is not possible, at least not within the constraints of the present study. Given the inherent limitation of the rainbow-ladder framework to pure vector-type interactions one may expect that corrections beyond rainbow ladder play an important role in this and other channels and may change this picture. Or it may simply be that the $X(3872)$ does indeed not have a strong quark-antiquark component. From the perspective of our framework, these questions remain open.

Clearly, the findings of this work should be corroborated by studies beyond the simple rainbow-ladder scheme used in this work. Within the light meson sector several approaches in this direction have been explored in the past [43–48] and it remains to be seen whether these can be transferred to the heavy quark sector. This will be the subject of future work.

We thank Gernot Eichmann, Maria Gomez-Rocha, Walter Heupel, Carina Popovici and Helios Sanchis-Alepuz for useful discussions. This work was supported by the BMBF under contract No. 06GI7121, the Helmholtz International Center for FAIR within the LOEWE program of the State of Hesse, and the Austrian Science Fund (FWF) under project number M1333-N16.

References

1. N. Brambilla, S. Eidelman, B.K. Heltsley, R. Vogt, G.T. Bodwin, E. Eichten, A.D. Frawley, A.B. Meyer *et al.*, *Eur. Phys. J. C* **71**, 1534 (2011) arXiv:1010.5827 [hep-ph].
2. G.V. Pakhlova, P.N. Pakhlov, S.I. Eidelman, *Phys. Usp.* **53**, 219 (2010) (*Usp. Fiz. Nauk* **180**, 225 (2010)).
3. for the BESIII Collaboration (J. Messchendorp), arXiv:1306.6611 [hep-ex].
4. G.T. Bodwin, E. Braaten, E. Eichten, S.L. Olsen, T.K. Pedlar, J. Russ, arXiv:1307.7425 [hep-ph].
5. S. Godfrey, N. Isgur, *Phys. Rev. D* **32**, 189 (1985).
6. D. Ebert, R.N. Faustov, V.O. Galkin, *Phys. Rev. D* **67**, 014027 (2003) hep-ph/0210381.
7. D. Ebert, R.N. Faustov, V.O. Galkin, *Eur. Phys. J. C* **71**, 1825 (2011) arXiv:1111.0454 [hep-ph].
8. F.J. Llanes-Estrada, O.I. Pavlova, R. Williams, *Eur. Phys. J. C* **72**, 2019 (2012) arXiv:1111.7087 [hep-ph].
9. Y. Koma, M. Koma, H. Wittig, *Phys. Rev. Lett.* **97**, 122003 (2006) hep-lat/0607009.
10. Y. Koma, M. Koma, *Nucl. Phys. B* **769**, 79 (2007) hep-lat/0609078.
11. N. Brambilla, A. Pineda, J. Soto, A. Vairo, *Rev. Mod. Phys.* **77**, 1423 (2005) hep-ph/0410047.
12. PACS-CS Collaboration (Y. Namekawa *et al.*), *Phys. Rev. D* **84**, 074505 (2011) arXiv:1104.4600 [hep-lat].
13. G.S. Bali, S. Collins, C. Ehmann, *Phys. Rev. D* **84**, 094506 (2011) arXiv:1110.2381 [hep-lat].
14. Hadron Spectrum Collaboration (L. Liu *et al.*), *JHEP* **07**, 126 (2012) arXiv:1204.5425 [hep-ph].
15. G. Moir, M. Peardon, S.M. Ryan, C.E. Thomas, L. Liu, *JHEP* **05**, 021 (2013) arXiv:1301.7670 [hep-ph].
16. M. Kalinowski, M. Wagner, *Acta Phys. Pol. B Proc. Suppl.* **6**, 991 (2013) arXiv:1304.7974 [hep-lat].
17. S. Prelovsek, L. Leskovec, *Phys. Rev. Lett.* **111**, 192001 (2013) arXiv:1307.5172 [hep-lat].
18. S. Prelovsek, L. Leskovec, D. Mohler, arXiv:1310.8127 [hep-lat].
19. D. Mohler, arXiv:1209.5790 [hep-lat].
20. S. Prelovsek, arXiv:1310.4354 [hep-lat].
21. M.S. Bhagwat, P. Maris, *Phys. Rev. C* **77**, 025203 (2008) nucl-th/0612069.
22. M. Blank, A. Krassnigg, *Phys. Rev. D* **84**, 096014 (2011) arXiv:1109.6509 [hep-ph].
23. T. Hilger, C. Popovici, M. Gomez-Rocha, A. Krassnigg, arXiv:1409.3205 [hep-ph].
24. C. Popovici, T. Hilger, M. Gomez-Rocha, A. Krassnigg, arXiv:1407.7970 [hep-ph].
25. W. Heupel, G. Eichmann, C.S. Fischer, *Phys. Lett. B* **718**, 545 (2012) arXiv:1206.5129 [hep-ph].
26. C. Popovici, P. Watson, H. Reinhardt, *Phys. Rev. D* **81**, 105011 (2010) arXiv:1003.3863 [hep-th].
27. C. Popovici, P. Watson, H. Reinhardt, *Phys. Rev. D* **83**, 125018 (2011) arXiv:1103.4786 [hep-ph].
28. C. Popovici, C.S. Fischer, *Phys. Rev. D* **89**, 116012 (2014) arXiv:1403.5900 [hep-ph].
29. C.S. Fischer, S. Kubrak, R. Williams, *Eur. Phys. J. A* **50**, 126 (2014) arXiv:1406.4370 [hep-ph].
30. J.E. Villate, D.S. Liu, J.E. Ribeiro, P.J. de A. Bicudo, *Phys. Rev. D* **47**, 1145 (1993).
31. P. Maris, P.C. Tandy, *Phys. Rev. C* **60**, 055214 (1999) nucl-th/9905056.
32. R. Williams, arXiv:1404.2545 [hep-ph].
33. R. Alkofer, W. Detmold, C.S. Fischer, P. Maris, *Phys. Rev. D* **70**, 014014 (2004) hep-ph/0309077.
34. C.S. Fischer, D. Nickel, R. Williams, *Eur. Phys. J. C* **60**, 47 (2009) arXiv:0807.3486 [hep-ph].
35. S.M. Dorkin, L.P. Kaptari, T. Hilger, B. Kampfer, *Phys. Rev. C* **89**, 034005 (2014) arXiv:1312.2721 [hep-ph].
36. A.C. Aguilar, D. Binosi, D. Ibanez, J. Papavassiliou, *Phys. Rev. D* **89**, 085008 (2014) arXiv:1312.1212 [hep-ph].
37. A. Blum, M.Q. Huber, M. Mitter, L. von Smekal, *Phys. Rev. D* **89**, 061703 (2014) arXiv:1401.0713 [hep-ph].
38. G. Eichmann, R. Williams, R. Alkofer, M. Vujanovic, *Phys. Rev. D* **89**, 105014 (2014) arXiv:1402.1365 [hep-ph].
39. A. Cucchieri, A. Maas, T. Mendes, *Phys. Rev. D* **77**, 094510 (2008) arXiv:0803.1798 [hep-lat].
40. E. Rojas, B. El-Bennich, J.P.B.C. de Melo, arXiv:1407.3598 [nucl-th].
41. M. Gomez-Rocha, T. Hilger, A. Krassnigg, arXiv:1408.1077 [hep-ph].
42. M.S. Bhagwat, A. Holl, A. Krassnigg, C.D. Roberts, P.C. Tandy, *Phys. Rev. C* **70**, 035205 (2004) nucl-th/0403012.
43. P. Watson, W. Cassing, P.C. Tandy, *Few-Body Syst.* **35**, 129 (2004) hep-ph/0406340.
44. C.S. Fischer, P. Watson, W. Cassing, *Phys. Rev. D* **72**, 094025 (2005) hep-ph/0509213.
45. C.S. Fischer, R. Williams, *Phys. Rev. D* **78**, 074006 (2008) arXiv:0808.3372 [hep-ph].
46. C.S. Fischer, R. Williams, *Phys. Rev. Lett.* **103**, 122001 (2009) arXiv:0905.2291 [hep-ph].
47. L. Chang, C.D. Roberts, *Phys. Rev. Lett.* **103**, 081601 (2009) arXiv:0903.5461 [nucl-th].
48. W. Heupel, T. Goecke, C.S. Fischer, *Eur. Phys. J. A* **50**, 85 (2014) arXiv:1402.5042 [hep-ph].